A Peptide-Tethered Lipid Bilayer on Mercury as a Biomimetic System

ARTICLE *in* LANGMUIR · OCTOBER 2001

Impact Factor: 4.46 · DOI: 10.1021/la010604w

6 AUTHORS, INCLUDING:

Cristina Peggion
University of Padova
133 PUBLICATIONS **2,134** CITATIONS
SEE PROFILE

Lucia Becucci
University of Florence
72 PUBLICATIONS **1,376** CITATIONS
SEE PROFILE

Maria Rosa Moncelli
University of Florence
121 PUBLICATIONS **2,053** CITATIONS
SEE PROFILE

Rolando Guidelli
University of Florence
226 PUBLICATIONS **3,904** CITATIONS
SEE PROFILE

A Peptide-Tethered Lipid Bilayer on Mercury as a Biomimetic System

Cristina Peggion, Fernando Formaggio, and Claudio Toniolo

Biopolymer Research Center, CNR, Department of Organic Chemistry, Padova University, 35131 Padova, Italy

Lucia Becucci, Maria Rosa Moncelli, and Rolando Guidelli*

Department of Chemistry, Florence University, Via G. Capponi 9, 50121 Florence, Italy

Received April 25, 2001. In Final Form: July 9, 2001

A novel spacer consisting of a hexapeptide molecule with a high tendency to form a 3_{10}-helical structure, which terminates with a sulfydryl group for anchoring to a metal, was tailored for use as a tethered hydrophilic spacer to be interposed between a metal support and a lipid bilayer. The thiol peptide has two triethylenoxy side chains that impart it a satisfactory hydrophilicity and are intended to keep the anchored thiol peptide chains sufficiently apart so as to accommodate water molecules and inorganic ions and to create a suitable environment for the incorporation of integral proteins. This thiol peptide was anchored to a hanging mercury drop electrode. The formation of a phospholipid bilayer on top of the self-assembled thiol peptide was carried out by a novel procedure which exploits the spontaneous tendency of a lipid film to form a bilayer when interposed between two hydrophilic phases. The resulting mercury-supported thiol peptide/lipid bilayer system was characterized by ac voltammetry with phase resolution, chronocoulometry, and impedance spectroscopy. The suitability of this tethered film as a biomembrane model was tested by incorporating ubiquinone-10 and valinomycin.

Introduction

So far, the experimental models of biomembranes that have been more extensively investigated are the *black lipid membranes* (BLMs).[1,2] BLMs are not suitable for biosensor technology since they are extremely fragile, metastable systems. Moreover, they do not lend themselves to investigations with surface-sensitive techniques. In an effort to overcome the drawbacks of conventional BLMs, metal-supported lipid monolayers and bilayers have been devised. They are normally obtained by self-assembly, which can be driven exclusively by noncovalent, hydrophobic interactions or with the additional contribution of covalent linkages. A simple and easily prepared biomembrane model obtained by noncovalent self-assembly consists of a phospholipid monolayer supported on a hanging mercury drop electrode.[3−6] Great interest has been focused on self-assembled films that are attached to a solid support by formation of a covalent linkage between the self-assembled molecules and the metal support, yielding structures of long-term, mechanical stability. Monolayers of alkanethiols on gold are probably the most widely used and best characterized of all self-assembled films to date.[7,8] Self-assembly involves the anchoring of the thiol to the gold surface through the sulfydryl group. The deposition of a phospholipid monolayer on top of a chemisorbed alkanethiol monolayer is normally accomplished by immersing a thiol-coated electrode into a dispersion of small lipid vesicles.[9−11] The spherical lipid bilayer of the vesicle must split to allow the hydrocarbon tails of the lipid to get in contact with those of the alkanethiol.

The possibility of covalently self-assembling bilayers on metals with formation of rugged functionalized electrodes has stimulated a research aiming at exploiting self-assembly for the realization of biomembrane models capable of incorporating integral proteins in a functionally active state. This approach has potential not only for fundamental research on protein functions but also for biosensor applications. To achieve this goal, biomembrane models consisting of lipid bilayers should be as flexible as lipid films in the liquid crystalline state, they should have an aqueous solution on both sides of the lipid bilayer, and they should be sufficiently free from pinholes and other defects that might provide preferential pathways for electron and ion transport across the lipid bilayer.[12] Metal-supported alkanethiol/phospholipid bilayers are unsuitable for incorporation of integral proteins because they lack flexibility and fluidity and because no hydrophilic layer is interposed between the bilayer and the electrode surface, thus excluding the space and water required for the proper folding of the extramembrane parts of integral proteins.

* Corresponding author. Tel.: 39-055-2757540. Fax: 39-055-244102. E-mail: guidelli@unifi.it.

(1) Mueller, P.; Rudin, D. O.; Tien, H. T.; Wescot, W. D. *Nature* **1962**, *194*, 979.
(2) Montal, M.; Mueller, P. *Proc. Natl. Acad. Sci. U.S.A.* **1972**, *69*, 3561.
(3) Nelson, A.; Benton, A. *J. Electroanal. Chem.* **1986**, *202*, 253.
(4) Moncelli, M. R.; Becucci, L.; Guidelli, R. *Biophys. J.* **1994**, *66*, 1969.
(5) Moncelli, M. R.; Becucci, L.; Nelson, A.; Guidelli, R. *Biophys. J.* **1996**, *70*, 2716.
(6) Moncelli, M. R.; Becucci, L.; Tadini Buoninsegni, F.; Guidelli, R. *Biophys. J.* **1998**, *74*, 2388.
(7) Nuzzo, R. G.; Fusco, F. A.; Allara, D. L. *J. Am. Chem. Soc.* **1987**, *109*, 2359.
(8) Porter, M. D.; Bright, T. B.; Allara, D. L.; Chidsey, C. E. D. *J. Am. Chem. Soc.* **1987**, *109*, 3559.
(9) Plant, A. L.; Gueguetchkeri, M.; Yap, W. *Biophys. J.* **1994**, *67*, 1126.
(10) (a) Williams, L. M.; Evans, S. D.; Flynn, T. M.; Marsh, A.; Knowles, P. F.; Bushby, R. J.; Boden N. *Langmuir* **1997**, *13*, 751. (b) Williams, L. M.; Evans, S. D.; Flynn, T. M.; Marsh, A.; Knowles, P. F.; Bushby, R. J.; Boden N. *Supramol. Sci.* **1997**, *4*, 513.
(11) Plant, A. L. *Langmuir* **1999**, *15*, 5128.
(12) Guidelli, R.; Aloisi, G.; Becucci, L.; Dolfi, A.; Moncelli, M. R.; Tadini Buoninsegni, F. *J. Electroanal. Chem.* **2001**, *504*, 1.

10.1021/la010604w CCC: $20.00
Published on Web 09/18/2001

In an attempt to overcome the above limitations, the alkanethiol monolayer has been replaced by a monolayer of "thiolipids", namely phospholipid molecules whose polar heads are covalently linked to a hydrophilic ethylenoxy[10,13−17] or oligopeptide[18−20] chain terminated with an anchoring thiol group, responsible for the chemisorption on gold. The hydrophilic chain anchored to the gold acts as a hydrophilic spacer interposed between the electrode surface and the phospholipid monolayer. A second phospholipid monolayer is then deposited on top of the first from a suspension of phospholipid vesicles, which split and spread on the thiolipid monolayer. Another procedure used to prepare spacer/bilayer assemblies on electrodes consists of anchoring a polyethylenoxy hydrophilic spacer to the electrode surface via a terminal sulfydryl group and in exposing the spacer-coated electrode to a suspension of small unilamellar vesicles[10,21,22]. In this case the bilayer formation on top of the monolayer of the hydrophilic spacer requires the rupture of the vesicles and their "unrolling" and spreading onto the spacer, without their splitting into two lipid monolayers. Thiolipids and hydrophilic spacers have been successfully anchored on gold and used to incorporate integral proteins by splitting or spreading of proteoliposomes[18−20,23−26]. So far, with these approaches, some difficulties have been encountered in obtaining metal-supported lipid bilayers free of pinholes and other defects; their presence is revealed by capacitances somewhat higher and resistances notably lower than those of solvent-free BLMs. This may cause the electrical signal following the activation of any electrogenic integral proteins incorporated in the metal-supported lipid bilayer to be notably disturbed by background noise.

The present work describes the use of a novel spacer consisting of a hexapeptide molecule with a high tendency to form a 3_{10}-helical structure, which terminates with a sulfydryl group for anchoring to the metal (Figure 1). This thiol peptide has two triethylenoxy side chains that impart it a satisfactory hydrophilicity and are intended to keep the anchored thiol peptide chains sufficiently apart so as to accommodate water molecules and inorganic ions and to create a suitable environment for the incorporation of integral proteins. This thiol peptide was anchored to a hanging mercury drop electrode. Mercury shares with gold a strong affinity for sulfydryl groups[27] but has the advantage of being readily renewable and of providing a defect-free surface to the self-assembling film. The formation of a phospholipid bilayer on top of the self-assembled thiol peptide was carried out by a novel procedure which exploits the spontaneous tendency of a lipid film to form a bilayer when interposed between two hydrophilic phases:[12,28,29] in the present case the lipid film was first spread on the surface of an aqueous electrolyte and then interposed between the latter and a mercury drop coated with the hydrophilic thiol peptide. The resulting mercury-supported thiol peptide/lipid bilayer system was characterized by ac voltammetry with phase resolution, chronocoulometry, and impedance spectroscopy. The suitability of this tethered film as a biomembrane model was tested by incorporating ubiquinone-10 and valinomycin.

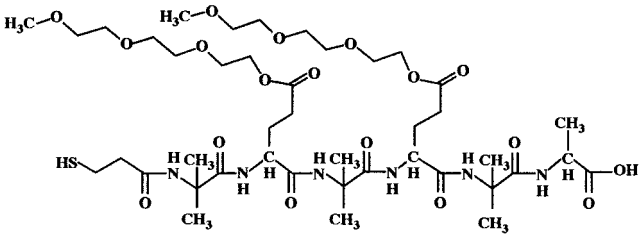

Figure 1. Chemical structure of the synthesized thiol peptide.

Experimental Section

Thiol Peptide Synthesis and Characterization. Melting points were determined using a Leitz model Laborlux 12 apparatus and are not corrected. Optical rotations were measured using a Perkin-Elmer model 241 polarimeter equipped with a Haake model D thermostat. Thin-layer chromatography (TLC) was performed on Merck Kieselgel 60-F254 precoated plates using the following solvent systems: (I) $CHCl_3$/EtOH, 9:1; (II) *n*BuOH/AcOH/H_2O, 3:1:1; (III) toluene/EtOH, 7:1. The chromatograms were developed by quenching of UV fluorescence, chlorine−starch−potassium iodide or ninhydrin chromatic reaction as appropriate. All compounds were obtained on a chromatographically homogeneous state. Analytical HPLC runs were performed on a Pharmacia model LKB-LCC 2252 liquid chromatograph equipped with an UVICORD model SD UV detector (226 nm) and a reverse-phase C_{18} Vydac model 218 TP54 column.

The synthesis of the thiol peptide $HS(CH_2)_2$[Aib-Glu(OTeg)]$_2$-Aib-Ala-OH (Aib, α-aminoisobutyric acid; Teg, triethylene glycol monomethyl ether), henceforth referred to as TP, was performed step-by-step in methylene chloride solution beginning from the C-terminal dipeptide ester H-Aib-Ala-O*t*Bu (O*t*Bu, *tert*-butoxy) [the latter obtained by catalytic hydrogenation of the corresponding, known N^{α}-benzyloxycarbonyl (Z) protected dipeptide ester[30] in methanol] via the racemization-free, *N*-ethyl-*N*′-(3-dimethylamino)propylcarbodiimide/1-hydroxy-7-aza-1,2,3-benzotriazole carboxyl activation method.[31] The Aib and Ala N^{α}-Z protected derivatives were obtained by reacting the pertinent free amino acid with Z-OSu (1-hydroxysuccinimide ester[32]). The Glu γ-carboxyl function was protected using commercial Z-Glu-O*t*Bu dicyclohexylammonium salt and the solubilizing alcohol triethylene glycol monomethyl ether (Teg-OH) in the presence of the carbodiimide mentioned above, 1-hydroxy-1,2,3-benzotriazole,[33] and *N*,*N*-dimethylaminopyridine.[34] Protection of the

(13) Lang, H.; Duschl, C.; Vogel, H. *Langmuir* **1994**, *10*, 197.
(14) Duschl, C.; Liley, M.; Corradin, G.; Vogel, H. *Biophys. J.* **1994**, *67*, 1229.
(15) Steinem, C.; Janshoff, A.; von dem Bruch, K.; Reihs, K.; Goossens, J.; Galla, H.-J. *Bioelectrochem. Bioenerg.* **1998**, *45*, 17.
(16) Raguse, B.; Braach-Maksvytis, V.; Cornell, B. A.; King, L. G.; Osman, P. D. J.; Pace, R. J.; Wieczorek, L. *Langmuir* **1998**, *14*, 648.
(17) Cornell, B. A.; Braach-Maksvytis, V. L. B.; King, L. G.; Osman, P. D. J.; Raguse, B.; Wieczorek, L.; Pace, R. J. *Nature* **1997**, *387*, 580.
(18) Naumann, R.; Jonczyk, A.; Kopp, R.; van Esch, J.; Ringsdorf, H.; Knoll, W.; Gräber, P. *Angew. Chem., Int. Ed.. Engl.* **1995**, *34*, 2056.
(19) Naumann, R.; Jonczyk, A.; Hampel, C.; Ringsdorf, H.; Knoll, W.; Bunjes, N.; Gräber, P. *Bioelectrochem. Bioenerg.* **1997**, *42*, 241.
(20) Bunjes, N.; Schmidt, E. K.; Jonczyk, A.; Rippmann, F.; Beyer, D.; Ringsdorf, H.; Gräber, P.; Knoll, W.; Naumann, R. *Langmuir* **1997**, *13*, 6188.
(21) Toby, A.; Jenkins, A.; Bushby, R. J.; Boden, N.; Evans S. D.; Knowles, P. F.; Liu, Q.; Miles, R. E.; Ogier, S. D. *Langmuir* **1998**, *14*, 4675.
(22) Steinem, C.; Janshoff, A.; Ulrich, W. P.; Sieber, M.; Galla, H.-J. *Biochim. Biophys. Acta* **1996**, *1279*, 169.
(23) Heyse, S.; Ernst, O. P.; Dienes, Z.; Hofmann, K. P.; Vogel, H. *Biochemistry* **1998**, *37*, 507.
(24) Schmidt, E. K.; Liebermann, T.; Kreiter, M.; Jonczyk, A.; Naumann, R.; Offenhäusser, A.; Neumann, E.; Kukol, A.; Maelicke, A.; Knoll, W. *Biosens. Bioelectron.* **1998**, *13*, 585.
(25) Heyse, S.; Stora, T.; Schmid, E.; Lakey, J. H.; Vogel, H. *Biochim. Biophys. Acta* **1998**, *85507*, 319.
(26) Naumann, R.; Schmidt, E. K.; Jonczyk, A.; Fendler, K.; Kadenbach, B.; Liebermann, T.; Offenhäusser, A.; Knoll, W. *Biosens. Bioelectron.* **1999**, *14*, 651.
(27) Tadini Buoninsegni, F.; Herrero, R.; Moncelli, M. R. *J. Electroanal. Chem.* **1998**, *452*, 33.
(28) Wardak, A.; Tien, H. T. *Bioelectrochem. Bioenerg.* **1990**, *24*, 1.
(29) Martynski, T.; Tien, H. T. *Bioelectrochem. Bioenerg.* **1991**, *25*, 317.
(30) Leibfritz, D.; Haupt, E.; Dubischar, N.; Lachmann, H.; Oekomomopulos, R.; Jung, G. *Tetrahedron* **1982**, *38*, 2165.
(31) Carpino, L. A. *J. Am. Chem. Soc.* **1993**, *115*, 4397.
(32) Frankel, M.; Ladkany, D.; Gilon, C.; Wolman, Y. *Tetrahedron Lett.* **1966**, 4765.
(33) König, W.; Geiger, R. *Chem. Ber.* **1970**, *103*, 788.
(34) Scriven, E. F. V. *Chem. Soc. Rev.* **1983**, 129.

Table 1. Physical and Analytical Properties for the Newly Synthesized, Protected Amino Acid Derivatives and Peptides Discussed in This Work

compd	yield (%)	mp (°C)	crystallization solvent	$[\alpha]_D^{20}$ [b] (deg)	TLC R_f(I)	TLC R_f(II)	TLC R_f(III)	IR (KBr) (cm^{-1})
Z-Glu(OTeg)-O*t*Bu	96	oil		−17.7	0.95	0.85	0.40	3339, 1734, 1608, 1587, 1526
Z-Glu(Oteg)-OH	70	oil		−8.4	0.90	0.85	0.20	3320, 1732, 1587, 1530
Z-Glu(OTeg)-Aib-Ala- O*t*Bu	57	oil		−33.0	0.90	0.80	0.20	3320, 1734, 1676, 1586, 1530
Z-Aib-Glu(OTeg)-Aib- Ala-O*t*Bu	85	oil		−20.0	0.85	0.80	0.10	3318, 1733, 1706, 1667, 1587, 1531
Z-Glu(OTeg)-Aib-Glu(OTeg)-Aib-Ala-O*t*Bu	52	oil		−14.4	0.85	0.70	0.10	3318, 1736, 1666, 1586, 1534
Z-[Aib-Glu(OTeg)]$_2$-A ib-Ala-OtBu	77	94−96	CH_2Cl_2 /PE[a]	−11.4	0.90	0.70	0.10	3322, 1736, 1703, 1663, 1531
Trt-S$(CH_2)_2$-[Aib-Gl u(OTeg)]$_2$-Aib-Ala-Ot Bu	68	oil		−2.0[c]	0.90	0.75	0.05	3312, 1736, 1658, 1596, 1534
HS$(CH_2)_2$-[Aib-Glu(OTeg)]$_2$-Aib-Ala-OH	55	oil		−3.6[c]	0.05	0.30	0.00	3327, 1733, 1657, 1563, 1534

[a] PE = petroleum ether. [b] Concentration = 0.5 (methanol). [c] $[\alpha]_{436}^{20}$.

thiol function of 3-mercaptopropionic acid was achieved by treatment of the free acid with trityl (Trt) chloride in methylene chloride in the presence of triethylamine. Removal of the −STrt and −O*t*Bu ester groups was simultaneously obtained in the final step by reacting the full protected hexapeptide with a 95: 2.5:2.5 solution of trifluoroacetic acid/water/triisopropylsilane.

Most of the synthetic intermediates were purified by flash-chromatography (ICN silica 32−63, 60 Å; eluant CH_2Cl_2/ethanol, 95:5), while the final product was purified by semipreparative HPLC (see above). The physical and analytical properties for the newly synthesized, protected amino acid derivatives and peptides are listed in Table 1. The final product was also characterized by ^{1}H NMR (400 MHz, dimethyl-d_6 sulfoxide; 20 °C): δ = 8.50 (s, 1H, Aib N*H*), 8.23 (d, 1H, N*H*), 7.77 (s, 1H, Aib N*H*), 7.49 (s, 1H, Aib N*H*), 7.37 (d, 1H, N*H*), 7.14 (d, 1H, N*H*), 4.22−4.05 (m, 7H, Ala αC*H*, 2 Glu αC*H*, 2 OTeg COOCH_2), 3.58−3.41 (m, 2OH, 10 OTeg CH_2), 3.23 (s, 6H, 2 OTeg CH_3), 2.89 and 2.59 [2m, 4H, S(CH_2)$_2$], 2.30−1.80 (m, 8H, 2 Glu βCH_2 and γCH_2), 1.37−1.29 (m, 18H, 6 Aib βCH_3), 1.35 (s, 9H, O*t*Bu CH_3), 1.21 (3H, d, Ala βCH_3).

FTIR Absorption. The FTIR absorption spectra were recorded using a Perkin-Elmer model 1720X spectrophotometer, nitrogen-flushed, equipped with a sample-shuttle device, at 2 cm^{-1} nominal resolution, averaging 100 scans. Solvent (baseline) spectra were obtained under the same conditions. Cells with path lengths of 0.1, 1.0, and 10.0 mm (with CaF_2 windows) were used. Spectrograde deuteriochloroform (99.8% D) was purchased from Fluka.

NMR Spectroscopy. The ^{1}H NMR spectra were recorded with a Bruker model AM 400 spectrometer. Measurements were carried out in deuterated dimethyl sulfoxide (DMSO) (99.96% D_6; Acros Organics).

Chemicals. The water used was obtained from light mineral water by distilling it once and by then distilling the water so obtained from alkaline permanganate. Merck suprapur KCl was baked at 500 °C before use to remove any organic impurities. Dioleoylphosphatidylcholine (DOPC) was obtained from Lipid Products (South Nutfield, Surrey, England). Valinomycin, gramicidin D, and horse-heart ubiquinone-10 (UQ) were purchased from Sigma and used without further purification. The other chemicals and solvents were also commercially available and were used as received. Pure DOPC and mixed DOPC/UQ solutions were prepared by dissolving in pentane a proper amount of stock solutions of DOPC and UQ. The percentage of UQ never exceeded 0.5 mol %. The 8×10^{-5} M solutions of the TP were prepared by dissolving in methanol/water (1:1) a proper amount of a 1×10^{-2} M stock solution of the compound in methanol; the methanol−water solutions were prepared weekly and stored at 4 °C under argon. In fact, the oxidation of thiols to disulfides was found to prevent a rapid and satisfactory covalent self-assembly on mercury. Stock solutions of 8×10^{-5} M valinomycin were prepared in chloroform and stored at 4 °C. To incorporate valinomycin in the lipid bilayer, small amounts of its stock solution were added to the aqueous electrolyte up to a maximum concentration of 10^{-7} M; the solution was then stirred gently for 20 min. The very small amounts of chloroform added to the aqueous solution ($\sim 10^{-3}$/L (v/v)) did not affect the electrochemical behavior either of the bare or of the coated mercury electrode. Among other things, chloroform is extremely insoluble in water and separates on the bottom of the cell. All measurements were carried out in 0.1 M KCl aqueous solutions buffered at pH 7−7.5 with a 1×10^{-3} M phosphate buffer except for the measurements with UQ, where a pH 8 borate buffer was employed.

Instrumentation. Use was made of a homemade hanging mercury drop electrode (HMDE) described elsewhere,[35] which allows changes in drop area of as little as 0.04 mm^2 to be estimated and highly reproducible drops to be obtained throughout the whole piston excursion. A homemade glass capillary with a finely tapered tip, about 1 mm in outer diameter, was employed. The capillary and the mercury reservoir were thermostated at 25 ± 0.1 °C by the use of a water-jacketed box to avoid any changes in drop area due to a change in temperature. A glass electrolysis cell containing the buffered solution of 0.1 M KCl and a small glass vessel containing the methanol−water solution of the TP were placed on a movable support inside the box, as shown in Figure 1 of ref 27. The vertical movements of the HMDE were obtained by means of an oleodynamic system, thus ensuring the complete absence of vibrations. A second oleodynamic system was used for the horizontal movements of the support, so as to bring the desired vessel just below the HMDE.

Differential capacitance and impedance spectroscopy measurements were carried out with an Autolab instrument (Echo Chemie) supplied with FRA2 module for impedance measurements, SCAN-GEN scan generator, and GPES3 software. Chronocoulometric measurements were carried out with a wholly computerized apparatus by following a procedure described elsewhere.[36,37] The microprocessor used to control all the operations was a model NOVA 4X from Data General (Westboro, MA), whereas an Amel model 551 (Milano, Italy) fast rise potentiostat with a rise time ≤0.5 μs was employed for the potentiostatic control of the three-electrode system. The chronocoulometric measurements consisted of a series of consecutive potential steps of progressively increasing width from a fixed initial value E_i, at which no faradaic processes are operative, to different final values E; each series was carried out on a single lipid-coated mercury drop. All potentials were measured vs a Ag|AgCl (0.1 M KCl) reference electrode and are referred to this electrode.

Electrode Functionalization. The procedure adopted to obtain a HMDE coated with the hydrophilic TP spacer and a DOPC bilayer on top of it consisted in keeping the mercury drop immersed in the small vessel containing the methanol/water (1:1) solution of 8×10^{-5} M TP for 30 min. In the meantime, a pentane solution of DOPC was spread on the surface of the aqueous 0.1 M KCl in the electrolysis cell in an amount corresponding to five to six DOPC monolayers, and the pentane was allowed to evaporate. Using the oleodynamic system, the TP-coated HMDE was then extracted from the vessel, the electrolysis cell was brought below the HMDE, and the latter was lowered so as to bring it into contact with the collapsed DOPC film, by taking care to keep the drop neck in contact with the lipid reservoir. This disposition allows a free exchange of material between the lipid-coated drop and the lipid reservoir on the surface of the aqueous electrolyte. The applied potential was then repeatedly scanned, first between −1.1 and −0.4 V and

(35) Moncelli, M. R.; Becucci, L. *J. Electroanal. Chem.* **1997**, *433*, 91.
(36) Foresti, M. L.; Moncelli, M. R.; Guidelli, R. *J. Electroanal. Chem.* **1980**, *109*, 1.
(37) Carla', M.; Sastre de Vicente, M.; Moncelli, M. R.; Foresti, M. L.; Guidelli, R. *J. Electroanal. Chem.* **1988**, *246*, 283.

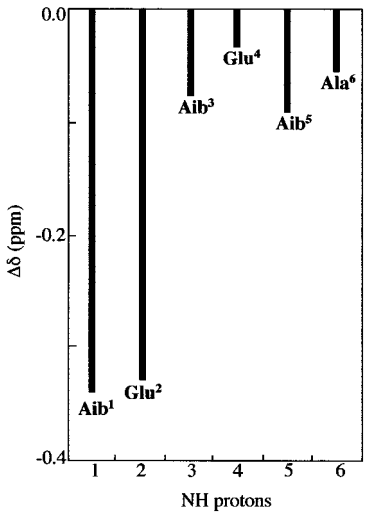

Figure 2. ^{1}H NMR titration of the fully protected hexapeptide Trt-S-$(CH_2)_2$-[Aib-Glu(OTeg)]$_2$-Aib-Ala-O*t*Bu. Plot of $\Delta\delta$(NH) chemical shifts as a function of increasing temperature (25−75 °C) in DMSO. Peptide concentration:1 mM.

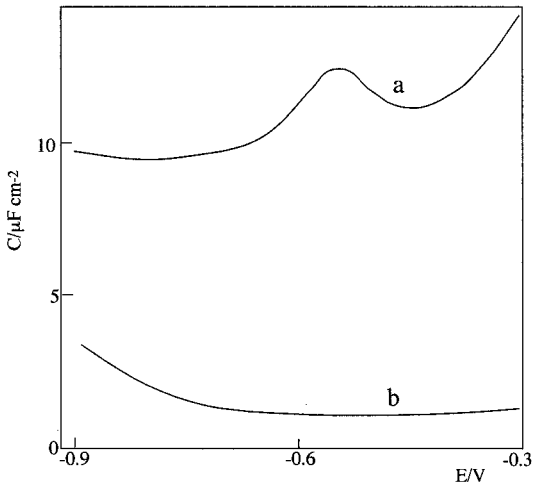

Figure 3. Plot of the differential capacitance, *C*, vs the applied potential, *E*, for TP-coated mercury (a) and for a DOPC film self-assembled on top of TP-coated mercury (b). Both curves were obtained in a 0.1 M KCl aqueous solution at a frequency of 75 Hz.

then between −0.8 and −0.4 V, while continuously monitoring the curve of the differential capacitance *C* vs the applied potential *E*, until a stable *C* vs *E* curve was attained. The impedance spectrum of the resulting lipid-coated electrode was recorded at −0.5 V, with a superimposed ac signal of 10 mV amplitude. The magnitude of the impedance $|Z(f)|$ and the phase angle $\phi(f)$ between voltage and current were recorded over the frequency range from 0.1 to 10^5 Hz. The *C* vs *E* curve and the impedance spectrum of the TP-coated HMDE were recorded by transferring the electrode from the TP containing vessel to the 0.1 M KCl solution, in the absence of the DOPC film on its surface.

Results and Discussion

Solution Conformational Analysis. A conformational analysis of the fully protected hexapeptide spacer Trt-S$(CH_2)_2$-[Aib-Glu(OTeg)]$_2$-Aib-Ala-O*t*Bu was performed using FTIR absorption and ^{1}H NMR in $CDCl_3$ and deuterated DMSO. In the 3500−3200 and 1800−1600 cm^{-1} regions the FTIR absorption spectrum in $CDCl_3$ solution (not shown) is dominated by strong bands at 3329 cm^{-1} (N−H stretching mode of H-bonded peptide groups) and 1667 cm^{-1} (C═O stretching mode of H-bonded peptide groups) .[38,39] Additional bands are seen at 3430 cm^{-1} (weak), assigned to free, solvated peptide N−H groups, and 1732 cm^{-1} (strong) and 1719 cm^{-1} (shoulder), assigned to OTeg and O*t*Bu ester carbonyls, respectively. In the N−H stretching region the peptide shows only a modest concentration effect (in the 5−0.1 mM concentration range), supporting the view that its secondary structure is highly folded and stabilized by an extensive set of intramolecular hydrogen bonds. The position of the strong C═O stretching band is also in favor of this conclusion.

To get more detailed information on the folded structure predominantly adopted by the hexapeptide in solution we carried out a ^{1}H NMR investigation. The analysis of inaccessible (or intramolecularly hydrogen-bonded) NH groups was performed by increasing the temperature of the peptide solution in the strong H-bonding acceptor DMSO .[40,41] Figure 2 illustrates the variation of the chemical shifts of the hexapeptide NH resonances under these conditions. All NH resonances were assigned by inspection of peak multiplicities and 2D NMR ROESY experiments.[42] Two classes of NH protons were found. (i) The first class [N(1)H and N(2)H protons] includes solvent-exposed protons, whose chemical shifts are remarkably sensitive to heating. (ii) The second class (all other NH protons) includes those displaying a behavior characteristic of shielded protons (relative insensitivity of the chemical shifts to heating). To summarize, these ^{1}H NMR results allow us to conclude that the N(3)H−N(6)H protons of the hexapeptide are almost inaccessible to the solvent and are therefore, most probably, intramolecularly hydrogen bonded. Thus, it is reasonable that the most populated conformation adopted in solution by the fully protected hexapeptide would be the 3_{10}-helix,[43] where only the two N-terminal NH protons do not participate in the intramolecular hydrogen-bonding scheme. This more detailed conformational conclusion is in full agreement with the indications extracted from the results of the FTIR absorption analysis discussed above and from literature data on the 3D-structural preference of Aib-based oligopeptides shorter than 7−8 residues.[44,45]

Differential Capacitance and Impedance Spectroscopy Measurements. Curve a in Figure 3 shows the *C* vs *E* plot for a TP film anchored to the mercury surface, as obtained at a frequency of 75 Hz after repeated scanning of the TP-coated mercury in aqueous 0.1 M KCl. A narrow capacitance minimum of about 9.5 μF cm^{-2} is observed at a potential of about −0.8 V. This relatively high capacitance value is comparable with those obtained with polypeptide monolayers on mercury[46,47] or with oligopeptides on gold.[48] It is reasonable to ascribe this value to the high polarizability of peptide bonds, thanks to their resonance hybrid structure in which the electron pair can move from the nitrogen to the oxygen atom and vice versa following the alternate electric field. A contribution to the polarizability of the film may also stem from a three-dimensional hydrogen-bonding network. Curve b

(38) Palumbo, M.; Da Rin, S.; Bonora, G. M.; Toniolo, C. *Makromol. Chem.* **1976**, *177*, 1477.
(39) Kennedy, D. F.; Crisma, M.; Toniolo, C.; Chapman, D. *Biochemistry* **1991**, *30*, 6541.
(40) Kopple, K. D.; Ohnishi, M. *Biochemistry* **1969**, *8*, 4087.
(41) Martin, D.; Hauthal, H. G. *Dimethyl Sulphoxide*; van Nostrand-Reinhold: Wokingham, U.K., 1975.
(42) Bax, A.; Davis, D. G. *J. Magn. Reson.* **1985**, *63*, 207.
(43) Toniolo, C.; Benedetti, E. *Trends Biochem. Sci.* **1991**, *16*, 350.
(44) Karle, I. L.; Balaram, P. *Biochemistry* **1990**, *29*, 6747.
(45) Toniolo, C.; Benedetti, E. *Macromolecules* **1991**, *24*, 4004.
(46) Miller, I. R.; Rishpon, J. In *Electrical Phenomena at the Biological Membrane Level*; Roux, E., Ed.; Elsevier: Amsterdam, 1977.
(47) Miller, I. R.; Bach, D.; Teuber, M. *J. Membr. Biol.* **1978**, *39*, 49.
(48) Naumann, R. Personal communication.

in Figure 3 shows the C vs E plot for a DOPC film self-assembled on top of the TP monolayer. Here the capacitance attains a flat minimum of about 1 μF cm^{-2} over the potential range from -0.3 to -0.7 V. This minimum is close to the capacitance value, 0.8 μF cm^{-2}, of a solvent-free black lipid membrane,[2] strongly suggesting that the lipid film is actually a bilayer freely suspended on top of the TP monolayer, with the polar heads directed toward both the aqueous phase and the hydrophilic spacer. The spontaneous tendency of a thick lipid film interposed between two hydrophilic phases to form a bilayer is well-known. Thus, it has been successfully employed in the preparation of bilayer lipid membranes (BLMs), which are formed by progressive thinning of a drop of a lipid solution in decane placed on a small hole in a Teflon septum separating two aqueous solutions. The excess of lipid material accumulates on the edge of the BLM so formed. A similar spontaneous phenomenon has also been exploited in the preparation of lipid bilayers supported by a hydrophilic Au, Ag, or steel electrode. In this case the lipid bilayer is obtained by cutting the end of a Teflon-coated hydrophilic metal wire while keeping it dipped in a decane solution of the lipid and by then immersing the freshly cut metal surface in an aqueous solution for 5−10 min for the lipid bilayer to self-assemble.[28,29] During this period the excess lipid solution creeps between the metal wire and its Teflon coating leaving a self-assembled bilayer on the metal surface. In the present case, the hydrophobic bare mercury surface is converted into a hydrophilic one upon coating with the hydrophilic TP. An advantage of mercury over freshly cut Au or Ag is represented by its defect-free surface; moreover, the lipid bilayer formed by the present procedure is free of the alkane solvent. To our knowledge, this is the first case in which a thiol peptide spacer interposed between a metal substrate and a lipid film yields a minimum differential capacitance as low as 1 μF cm^{-2}. Thus, C values ranging from 3 [19] to 15 [26] have been reported on a gold substrate. More satisfactory capacitance values, in the range of 0.5−0.7 μF cm^{-2}, were obtained with polyethylenoxy hydrophilic spacers on gold.[13] A higher value of 1 μF cm^{-2} was reported for longer spacers.[15] Moreover, a lipid bilayer with a capacitance of 0.5−0.6 μF cm^{-2} and a resistance $>5 \times 10^6$ Ω cm^2, which compare favorably with those of conventional BLMs, was obtained by placing a small quantity of a bilayer-forming lipid dissolved in ethanol onto a gold electrode coated with a mixture of short and long hydrophilic spacers; the lipid in excess with respect to that required for the bilayer was then rinsed away vigorously with an aqueous solution.[16]

The fairly satisfactory C value of about 1 μF cm^{-2} herein obtained with an oligopeptide spacer is to be ascribed to the defect-free Hg surface and to the mobility of the mercury surface atoms, which allow a gradual self-assembly of the TP monolayer and of the overhanging lipid film during the repeated potential scans. It should also be noted that the attainment of a capacitance as low as 1 μF cm^{-2} upon self-assembly of a lipid bilayer on top of a thiol peptide monolayer demands a fairly good compactness from the lipid bilayer; in fact, even relatively small lipid-free domains are expected to cause an appreciable increase in the overall differential capacitance, in view of the high capacitance value of the single TP monolayer. By gradual expansion of the area of the bilayer-coated mercury drop up to twice its initial value, no detectable change in capacitance was observed. This proves the free exchange of lipid material between the lipid-coated mercury and the lipid reservoir on the surface of the aqueous electrolyte; the unavoidable thinning of the flexible TP monolayer during such an expansion has no detectable effect, because the high capacitance of this monolayer makes a negligible contribution to the overall capacitance of the mixed film.

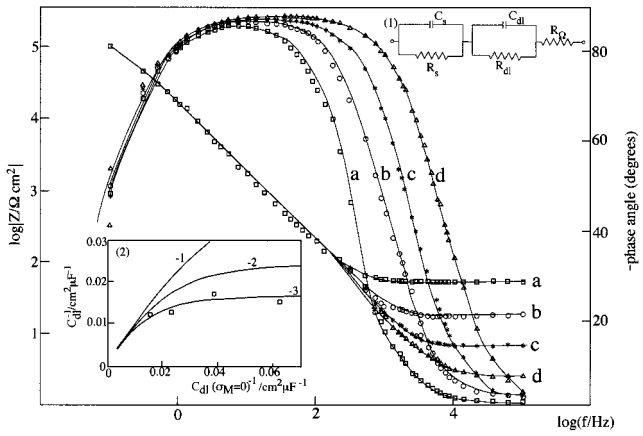

Figure 4. Plots of log $|Z|$ and ϕ vs log f for a TP-coated mercury drop immersed in 5×10^{-3} M (a), 1.3×10^{-2} M (b), 3.6×10^{-2} M (c), and 0.1 M (d) KCl, as obtained at -1.000 V over the frequency range from 0.1 to 10^5 Hz. At frequencies $<10^2$ Hz all Bode plots coincide; hence, only the experimental points for the lower KCl concentration were reported. The solid curves are least-squares fits to the simple equivalent circuit of inset 1, which consists of the electrolyte resistance R_Ω, with in series a R_sC_s mesh representing the self-assembled TP monolayer and a further $R_{dl}C_{dl}$ mesh representing the diffuse layer. $R_s =$ 0.14 MΩ cm^2, $C_s = 11$ μF cm^{-2}, and $R_{dl} = 4.53$ (a), 4.17 (b), 1.27 (c), and 0.87 KΩ cm^2 (d). $C_{dl} = 68$ (a), 61 (b), 80 (c), and 84 μF cm^{-2} (d). Inset 2 shows the reciprocal, $1/C_{dl}$, of the experimental diffuse-layer capacitance vs the $1/C_{dl}(\sigma_M = 0)$ value corresponding to the same KCl concentration, as calculated on the basis of the Gouy−Chapman (GC) theory. The solid curves are $1/C_{dl}(\sigma_M)$ vs $1/C_{dl}(\sigma_M = 0)$ plots calculated from the GC theory for different charge densities σ_M on the metal, whose values are reported on each curve.

Impedance spectroscopy has proved a valuable tool for the characterization of solid-supported films. Plots of log $|Z|$ vs log f (Bode plot) and of the phase angle ϕ vs log f at -1.000 V for TP-coated mercury in the presence of four different KCl concentrations are shown in Figure 4. The solid curves are least-squares fits to the simple equivalent circuit reported in inset 1 of the same figure: it consists of the electrolyte resistance R_Ω, with in series a R_sC_s mesh representing the self-assembled TP monolayer and a further $R_{dl}C_{dl}$ mesh representing the diffuse layer. The fitting was carried out by imposing the R_s and C_s circuit elements to remain constant with varying the electrolyte concentration. The resulting C_s value equals 11 μF cm^{-2}, in agreement with the value obtained from phase-sensitive ac voltammetry at 75 Hz, while R_s amounts to 0.14 MΩ cm^2. This relatively high resistance is typical of thiol peptide self-assembled monolayers[48] and denotes a good compactness of the tethered monolayer. However, it is much lower than the resistance of long-chain n-alkanethiol monolayers on Hg[27] and Au,[9] which are rigid and in the gel state. The solid curves in inset 2 of Figure 4 are plots of $1/C_{dl}(\sigma_M)$, calculated from the GC theory for different values of the charge density σ_M on the metal, as a function of the corresponding GC value at $\sigma_M = 0$, $1/C_{dl}(\sigma_M = 0) = 4.38 \times 10^{-3} c^{-1/2}$, where c is the KCl concentration in moles liter^{-1} and the differential capacitance is in μF cm^{-2}. This plot yields a straight line of unit slope for $\sigma_M = 0$ and curves of decreasing average slope with an increase in the absolute value of σ_M. The points in the same inset are values of the reciprocal, $1/C_{dl}$, of the experimental diffuse-layer capacitance against 4.38×10^{-3} $c^{-1/2}$. The experimental points are in fairly good agreement with the

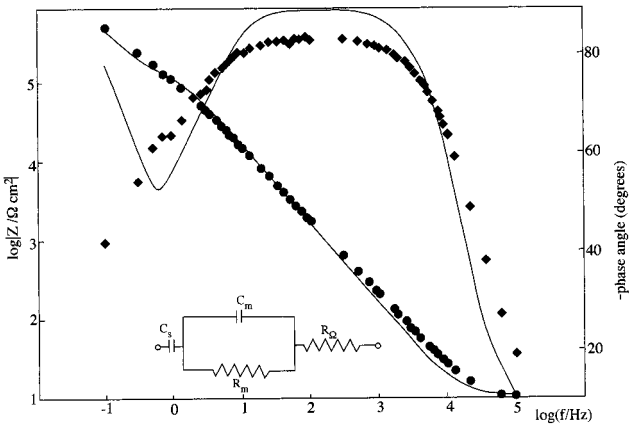

Figure 5. Plots of log $|Z|$ and ϕ vs log f for a DOPC bilayer self-assembled on top of TP-coated mercury, as obtained in aqueous 0.1 M KCl at −0.500 V over the frequency range from 0.1 to 10^5 Hz. The solid curves are least-squares fits to the equivalent circuit shown in the inset: $C_s = 4.2\ \mu$F cm^{-2}; $R_m = 0.09$ MΩ cm^2; $C_m = 1.1\ \mu$F cm^{-2}; $R_\Omega = 10$ Ω cm^2.

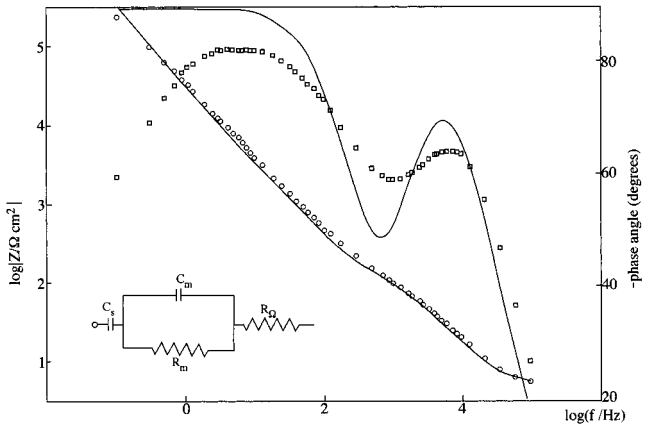

Figure 6. Plots of log $|Z|$ and ϕ vs log f for a DOPC bilayer self-assembled on top of TP-coated mercury, as obtained at −0.500 V in aqueous 0.1 M KCl containing 1×10^{-7} M valinomycin. The solid curves are least-squares fits to the same equivalent circuit as in Figure 5: $C_s = 4.5\ \mu$F cm^{-2}; $R_m = 90$ Ω cm^2; $C_m = 1.3\ \mu$F cm^{-2}; $R_\Omega = 7$ Ω cm^2.

calculated $1/C_{dl}(\sigma_M)$ vs $1/C_{dl}(\sigma_M = 0)$ plot corresponding to $\sigma_M = -3\ \mu$C cm^{-2}. However, it must be stressed that in the present case the charge of $-3\ \mu$C cm^{-2} is just the extrathermodynamic charge experienced by the diffuse-layer ions and not the thermodynamically significant charge density on the metal, because of partial charge transfer from sulfur to mercury (see below). Figure 5 shows plots of log $|Z|$ and ϕ vs log f for TP-coated mercury with a DOPC bilayer on top, at −0.500 V and in 0.1 M KCl. In this case the impedance spectrum was least-squares fitted to an equivalent circuit consisting of the capacitance C_s of the TP monolayer, with in series an R_mC_m mesh and the electrolyte resistance R_Ω ; the R_mC_m mesh accounts for the resistance R_m and the capacitance C_m of the lipid bilayer. The equivalent circuit does not include the $R_{dl}C_{dl}$ mesh of Figure 4, in view of the negligible contribution of this mesh to the impedance response in the presence of the very low capacitance, C_m, of the lipid film and of the relatively high 0.1 M KCl concentration. The fitting yields a C_m value of 1.1 μF cm^{-2} and a R_m value of 0.09 MΩ cm^2, confirming the formation of a self-assembled DOPC bilayer freely suspended on top of the TP spacer. It also yields a C_s value of 4.2 μF cm^{-2}, which is somewhat lower than the value, 11 μF cm^{-2}, obtained from Figure 4. It is not clear whether this relatively slight difference is real or is merely due to the use of a different equivalent circuit. The discrepancies between the ϕ vs log f plot and the fitted curve might be removed to a large extent by introducing constant phase elements (CPEs). However, these were not included in the equivalent circuit to avoid increasing the number of adjustable parameters and because of their dubious physical significance. At any rate, these discrepancies denote the presence of a few defects in the lipid bilayer (see below).

After ascertaining the formation of a lipid bilayer, it is important to verify whether the hydrophilic spacer may act as a satisfactory reservoir of water and inorganic ions, as required for the incorporation of integral proteins in a functionally active state. A simple but extremely useful test consists of incorporating in the lipid layer the ion carrier valinomycin and in verifying to what extent it increases the conductance of the biomembrane model.[15,16] The addition of valinomycin causes a notable change in the impedance spectrum, as appears from Figure 6. The Bode plot shows a small but appreciable inflection between two rectilinear sections of almost −1 slope at a frequency of about 10^3 Hz. Over the same frequency range the $\phi(f)$ vs log(f) plot shows a clear minimum between two capacitive maxima. An analogous behavior was reported by Steinem et al.[15] and Raguse et al..[16] The fitting of this Bode plot to the same equivalent circuit as in Figure 5 is not particularly good, although it might be considerably improved by replacing the capacitive elements by CPEs. At any rate, the fitting clearly shows that the addition of valinomycin causes a slight increase in the bilayer capacitance C_m from 1.1 to 1.3 μF cm^{-2} and a drastic decrease in its resistance R_m from 0.09 to 90 Ω cm^2. The calculated value for C_s is about 4.5 μF cm^{-2}. This behavior indicates that, as the frequency is progressively decreased approaching 10^3 Hz, the impedance control tends to pass from the C_m element to the R_m element, causing the slope of the Bode plot to approach the zero value. Before this can occur, however, the impedance control passes to the capacitive element C_s of the thiol peptide.

Partial Charge Transfer from the Thiol Peptide to Mercury. Chemisorption of the thiol peptide on mercury involves a partial charge transfer from the sulfur atom to mercury, as well as a partial deprotonation of the sulfydryl group. The partial charge transfer can be approximately estimated by measuring the thermodynamic "total" charge density σ_M on the metal, i.e. the charge density to be supplied to the electrode to keep the applied potential constant when the electrode surface is increased by unity; the extrathermodynamic "free" charge density q, i.e. the charge actually experienced by the diffuse layer ions, must also be estimated.[49] Let us denote the partial charge-transfer coefficient by λ and the degree of dissociation of the sulfydryl groups by α. Since partial electron transfer from the sulfydryl groups and their deprotonation are strictly correlated events, it is reasonable to regard λ and α as equal, as a first approximation. With this assumption, it can be shown that the overall charge experienced by the diffuse layer ions is given by $q = (\sigma_M + \lambda\sigma_i)$.[49] Here σ_i is the charge density that would correspond to total electron transfer from the sulfydryl group to mercury, i.e., $-eN$, where N is the number density of the chemisorbed TP molecules. The diameter d of the 3_{10}-helix of a TP molecule amounts to about 9.5 Å. Assuming that the adsorbed TP molecules form a close-packed hexagonal array, with the helix normal to the

(49) Tadini Buoninsegni, F.; Becucci, L.; Moncelli, M. R.; Guidelli, R. *J. Electroanal. Chem.* **2001**, *500*, 395.

electrode surface, their cross-sectional area equals $\sqrt{3}d^2/2 = 1/N = 78$ Å^2; hence, σ_i is approximately equal to -20 μC cm^{-2}.

The curves of the differential capacitance C vs E of a bare Hg electrode and of a TP-coated one, both immersed in the same 0.1 M tetramethylammonium chloride ((TMA)Cl) aqueous electrolyte, merge at potentials negative of -1.850 V, thus indicating that TP is completely desorbed at these far negative potentials. This allows the absolute charge density σ_M on TP-coated mercury to be readily determined over the whole potential range of stability of the TP monolayer by the procedure outlined in ref 49. Briefly, the charge involved in a chronocoulometric potential step on bare Hg from the potential of zero charge (pzc) of aqueous 0.1 M (TMA)Cl, -0.486 V,[50] to -1.900 V equals -24 μC cm^{-2}: it provides the charge density, σ_M (-1.900 V), at the latter potential both on bare and on TP-coated mercury. The charge $Q = \sigma_M(-1.900\ \text{V}) - \sigma_M(-1.000\ \text{V})$ following a potential step on TP-coated mercury from -1.000 to -1.900 V amounts to -41 μC cm^{-2}. The total charge density σ_M (-1.000 V) on TP-coated Hg at -1.000 V is, therefore, equal to $+17$ μC cm^{-2}. The charge density q (-1.000 V) experienced by the diffuse layer ions at -1.000 V on TP-coated mercury was already estimated from electrochemical impedance measurements (Figure 4) and amounts to -3 μC cm^{-2}. The partial charge-transfer coefficient $\lambda \approx (q - \sigma_M)/\sigma_i$ is, therefore, approximately equal to unity. This denotes an almost complete electron transfer from the sulfydryl group to mercury.

Electroreduction of Ubiquinone-10 Incorporated in the TP|DOPC Film. Ubiquinone-10 (UQ) is an important, ubiquitous biomolecule that is present in many membranes and acts as a proton and electron carrier in the respiratory chain of the mitochondrial membrane. It consists of a quinone ring, which can be reduced to the corresponding quinol, and is provided with a long, rigid isoprenoid chain imparting it a high affinity for lipids. The electrochemical behavior of pure UQ mono- or submonolayers deposited on a mercury electrode was investigated by Gordillo and Schiffrin,[51] while the electroreduction mechanism of UQ incorporated in a DOPC monolayer supported on mercury was investigated in the present laboratory both by chronocoulometry[5] and by cyclic voltammetry.[52] Briefly, UQ is reduced to ubiquinol-10 (UQH_2) via the reversible uptake of one electron, followed by the rate determining protonation of the resulting semiubiquinone radical, UQ^-. UQ reduction was not observed upon self-assembling a DOPC monolayer incorporating UQ on top of a *n*-octadecanethiol monolayer supported on Hg,[27] thus indicating that UQ molecules cannot permeate this monolayer, in view of its lack of fluidity. It was, therefore, of interest to verify whether UQ electroreduction can take place across the TP monolayer. To this end, 0.5 mol % UQ was incorporated in the collapsed lipid film spread on the surface of the aqueous electrolyte, a TP-coated mercury drop was then brought into contact with this film, and the applied potential was repeatedly scanned as described in the Experimental Section. The presence of UQ was found to increase the minimum differential capacitance of the film from ~1.0 to ~1.5 μF cm^{-2}. Subsequently, a series of chronocoulometric potential steps was carried out from a fixed initial potential $E_i = -0.1$ V to progressively more negative final potentials E, as described in ref 5. The charge $Q(t, E)$ following these potential steps was recorded as a function of time. Curve a in Figure 7 shows the charge density $Q(t = 100\ \text{ms}, E)$ flown after 100 ms from the instant of each potential step $E_i \rightarrow E$, against E. Curve b in the same figure shows the $Q(t = 100\ \text{ms}, E)$ vs E curve obtained by carrying out the same chronocoulometric measurements on a DOPC-coated mercury drop obtained as described in ref 5, by completely immersing a bare mercury drop into the aqueous electrolyte across the collapsed DOPC film incorporating UQ. The height of these sigmoidal curves, as measured by the vertical distance between their plateau and the linear extrapolation of their foot, is a measure of the amount of UQ incorporated in the lipid film. The height of curve a amounts to 0.5 μC cm^{-2}, in good agreement with the value estimated for a DOPC bilayer containing 0.5 mol % UQ, under the assumption that both the lipid and the UQ molecules occupy a surface area of 65 Å^2 and that UQ undergoes a two-electron reduction to UQH_2 (see Figure 2 in ref 5). The error made in ascribing to the UQ molecules the same surface area as the DOPC molecules is entirely negligible at this low UQ concentration. The height of curve b, obtained with a DOPC monolayer, is about half that of curve a. The amount of UQ in the lipid bilayer being twice that in the lipid monolayer is not to be regarded as obvious. In fact, in the case of the lipid monolayer, the UQ molecules are dragged into the bulk solution by the mercury drop together with the lipid molecules; therefore, the UQ concentration in the monolayer is prevented from changing with respect to that in the collapsed lipid film on the surface of the aqueous electrolyte.[5] On the other hand, the free exchange of material (including UQ molecules) between the lipid bilayer on top of the TP-coated mercury and the collapsed lipid film on the surface of the aqueous electrolyte allows the UQ molecules to equilibrate between the bilayer and the contacting collapsed film. Therefore, the amount of UQ in the bilayer being twice that in the monolayer indicates that the UQ molecules prefer to stay in the bilayer, probably with their long isoprenoid chain sandwiched between the two lipid monolayers, than in a lipid monolayer, probably in direct contact with the mercury

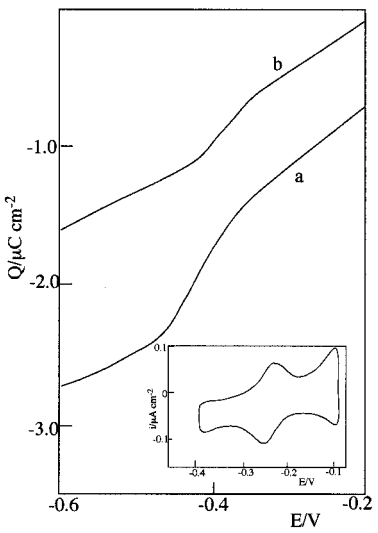

Figure 7. $Q(t = 100\ \text{ms}, E)$ vs E plots for UQ electroreduction obtained, as described in the text, by self-assembling DOPC containing 0.5 mol % UQ on top of TP-coated mercury (a) and on bare mercury (b) in a pH 8 buffered solution of 0.1 M KCl. The inset is the cyclic voltammogram obtained on the same electrode yielding curve a; scan rate = 5 mV/s.

(50) Kimmerle, F. M.; Ménard, H. *J. Electroanal. Chem.* **1974**, *54*, 101.

(51) Gordillo, G. J.; Schiffrin, D. *J. Chem. Soc., Faraday Trans.* **1994**, *90*, 1913.

(52) Moncelli, M. R.; Herrero, R.; Becucci, L.; Guidelli, R. *Biochim. Biophys. Acta* **1998**, *1364*, 373.

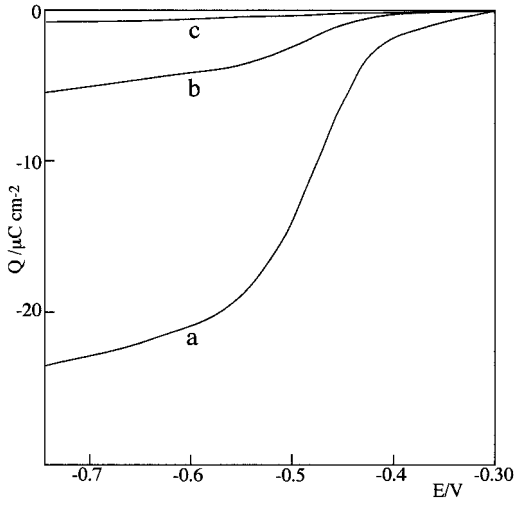

Figure 8. $Q(t = 100$ ms, $E)$ vs E plots for 10^{-4} M Tl^+ electroreduction from aqueous 0.1 M KCl on bare mercury (a), on TP-coated mercury with a DOPC monolayer on top (b), and on mercury coated with a DOPC monolayer (c).

surface. Curve a being more drawn out than curve b and shifted toward more negative potentials is to be ascribed to the ohmic drop across the TP spacer. The inset of Figure 7 shows the cyclic voltammogram of the DOPC bilayer incorporating UQ, as recorded at pH 8 with a scan rate of 5 mV s^{-1}. Both the reduction peak of UQ to UQH_2 and the corresponding oxidation peak are clearly visible, and the charge under both peaks is again equal to 0.5 μC cm^{-2}. Their peak potentials, −0.250 V and −0.230 V, are relatively close, denoting a quasi-reversible behavior of the UQ/UQH_2 redox couple at the low scan rate adopted. The midpoint potential, −0.240 V, measures the formal potential of this couple and agrees with the value, −0.230 V, obtained on a DOPC monolayer.[52] The above results indicate that the TP spacer anchored to Hg is fluid and flexible enough to be permeated by a hydrophobic molecule such as UQ.

Permeability of a TP|DOPC Film to Tl^+ Ions. A phospholipid monolayer self-assembled on a mercury electrode is practically impermeable to Tl^+ ions over a potential range from −0.2 to −0.7 V/SCE, even though Tl^+ ions is reduced reversibly on bare mercury with a formal potential of −0.457 V/SCE.[53] It was, therefore, of interest to verify the blocking effect of the lipid bilayer on top of the TP upon Tl^+ electroreduction. To this end, the potential-step chronocoulometric technique was adopted, by carrying out a series of potential steps from a fixed initial potential $E_i = -0.300$ V, at which Tl^+ ion is still electroinactive and the lipid bilayer is well organized, to progressively more negative potentials E. Curve b in Figure 8 shows a plot of the charge Q (100 ms, E), measured 100 ms from the instant of each potential step, against the applied potential E for 1×10^{-4} M Tl^+ electroreduction from aqueous 0.1 M KCl on TP-coated mercury with a DOPC bilayer on top. Curves a and c show Q (100 ms, E) vs E plots obtained on bare mercury and on mercury coated with a DOPC monolayer, under otherwise identical conditions. It is apparent that the blocking effect of the lipid bilayer is not complete, since a Tl^+ wave is observed, whose height is about one-fifth that of the diffusion-controlled wave on bare mercury. If we consider that the present lipid bilayer has a minimum capacitance of 1 μF cm^{-2}, as compared to that, ~0.8 μF cm^{-2}, of a solvent-free black lipid membrane, it is evident that its surface coverage, θ, is slightly less than unity. It is possible that the self-assembly of the lipid bilayer on top of the flexible, hydrophilic TP monolayer is less tight than that of a lipid monolayer on the hydrophobic bare mercury surface. Assuming that the fraction of lipid-free surface, $1 - \theta$, is filled with water molecules and ascribing to this fraction the minimum differential capacitance, 16 μF cm^{-2}, of a water-covered mercury surface, θ is estimated at $(16 - 1)/(16 - 0.8) = 99.67$. Despite this high surface coverage, the water-filled holes present in the lipid bilayer are sufficient to cause some penetration of Tl^+ ions.

Conclusions

An alternative to metal-supported mixed alkanethiol/phospholipid bilayers is described, which makes use of a novel, 3_{10}-helical thiol peptide anchored to a hanging mercury drop electrode. The thiol peptide was tailored for use as a tethered hydrophilic spacer to be interposed between a metal support and a lipid bilayer. A novel procedure for the deposition of a lipid bilayer on top of the thiol peptide-coated mercury, alternative to the fusion of lipid vesicles, is also proposed. The use of mercury in place of gold has the advantage of a readily renewable and defect-free surface, on which thio derivatives self-assembly more rapidly. The fluidity and impermeability of the mercury-supported thiol peptide monolayer with a phospholipid film on top were tested to assess its validity as an experimental model of biological membranes. Its response to the incorporation of valinomycin and ubiquinone-10 and its impedance spectrum indicate that this membrane model has a good fluidity and consists of a stable lipid bilayer on top of a hydrophilic spacer acting as an ionic reservoir. The partial blocking effect upon Tl^+ electroreduction points to a fairly, but not entirely, compact lipid bilayer.

Further research will be directed to the use of this thiol peptide on a gold substrate and to the condensation of its C-terminal carboxyl group with the amino group of dimyristoylphosphatidylethanolamine. The resulting thiolipid is expected to self-assemble on mercury or gold, giving rise to a lipid monolayer covalently linked to the tethered hydrophilic thiol peptide, on which a second lipid monolayer may be easily deposited by exploiting hydrophobic interactions.

Acknowledgment. The financial support of the Ministero dell'Universitá e della Ricerca Scientifica e Tecnologica and of the Consiglio Nazionale delle Ricerche (CNR) of Italy is gratefully acknowledged.

LA010604W

(53) Nelson, A. *J. Electroanal. Chem.* **1991**, *303*, 221.